Construction of Behavioral Models for Microwave Devices from Time Domain Large-Signal Measurements to Speed Up High-Level Design Simulations

D. Schreurs,[1] J. Wood,[2] N. Tufillaro,[3] L. Barford,[3] D. E. Root[2]

[1] Katholieke Universiteit Leuven, ESAT-TELEMIC, Kasteelpark Arenberg 10, B-3001 Leuven-Heverlee, Belgium
[2] Agilent Technologies, Microwave Technology Center, Santa Rosa, California 95403
[3] Agilent Laboratories, Palo Alto, California 94304

Received 11 January 2001; Accepted 29 April 2002

ABSTRACT: Behavioral models for microwave devices from time domain large-signal measurements are developed. For the presented examples, the model is defined by representing the terminal currents as a function of the terminal voltages and their derivatives. When using these models as building blocks of higher level designs, the simulation speed is significantly improved. © 2003 Wiley Periodicals, Inc. Int J RF and Microwave CAE 13: 54–61, 2003.

Keywords: microwave devices; large-signal measurements; device modeling; time series analysis; optimization

I. INTRODUCTION

The recent availability of vectorial large-signal measurement setups [1–4] makes it possible to develop new measurements based nonlinear modeling approaches that are not limited to the use of only static (DC) and *S*-parameter data. Some examples of such modeling techniques include parametric equivalent-circuit model extraction [5–7] and black-box model identifications in the frequency domain [7, 8].

In this work we develop a time domain black-box modeling procedure, which is based on nonlinear system identification, using techniques developed in nonlinear time-series analysis (NLTSA) [9–11]. One advantage of this technique is that the resulting model should be transportable; in other words, it should be usable in a range of environments and not restricted to a small domain of applicability, for example, a single bias condition. A further advantage of this time domain technique is that it is not restricted to the modeling of only weakly nonlinear phenomena, unlike some frequency domain methods such as Volterra series analysis. The model is described directly by time-differential equations that are reconstructed from measured data. By this means, all the observable dynamics of the device are determined. Finally, this black-box modeling principle is applicable to any device type, regardless of its complexity, because no physical preknowledge is required. Because only the observable dynamics are captured, the model size of circuits in particular will generally be significantly smaller compared to the case where these circuits are represented by separate models for each of the constituting building blocks. This enables the construction of a compact, accurate, and transportable dynamical model [12, 13].

In the next section we describe in detail the modeling procedure we developed. The different steps are

Correspondence to: Dr. D. Schreurs; e-mail: Dominique.Schreurs@esat.kuleuven.ac.be.
Contract grant sponsor: Agilent Technologies.
Published online in Wiley InterScience (www.interscience.wiley.com). DOI 10.1002/mmce.10062

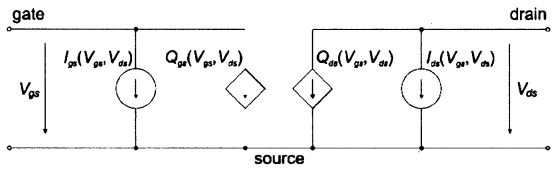

Figure 1. A simplified large-signal equivalent scheme of a HEMT.

clarified by applying them to a microwave transistor, a high electron mobility transistor (HEMT), and a monolithic integrated amplifier circuit (MMIC). The obtained models are validated by examining the DC, small-signal, and large-signal behavior (Section III). Finally, we give an indication about the gain in simulation time when using this type of model representation.

II. METHODOLOGY

To introduce the principle, we take HEMT as an example. Its simplified large-signal equivalent scheme is shown in Figure 1. We neglect the extrinsic parasitic network and the nonquasistatic effects to simplify the following equations. The terminal currents $I_1(t)$ and $I_2(t)$ can be expressed by

$$I_1 = I_{gs}(V_1(t), V_2(t)) + \frac{dQ_{gs}(V_1(t), V_2(t))}{dt}, \quad (1)$$

$$I_2 = I_{ds}(V_1(t), V_2(t)) + \frac{dQ_{ds}(V_1(t), V_2(t))}{dt}, \quad (2)$$

where $V_1(t)$ and $V_2(t)$ are the terminal voltages that correspond to voltages $V_{gs}(t)$ and $V_{ds}(t)$, respectively; and subscripts ds and gs are drain-source and gate source, respectively.

By taking the partial derivatives of the charges $Q_{gs}(t)$ and $Q_{ds}(t)$ toward the voltages $V_1(t)$ and $V_2(t)$, we obtain

$$I_1(t) = I_{gs}(V_1(t), V_2(t)) + C_{11}(V_1(t), V_2(t))\frac{dV_1(t)}{dt} + C_{12}(V_1(t), V_2(t))\frac{dV_2(t)}{dt}, \quad (3)$$

$$I_2(t) = I_{ds}(V_1(t), V_2(t)) + C_{21}(V_1(t), V_2(t))\frac{dV_1(t)}{dt} + C_{22}(V_1(t), V_2(t))\frac{dV_2(t)}{dt}, \quad (4)$$

or, in other words, the terminal currents are a function of the terminal voltages and the first derivatives of the terminal voltages:

$$I_1(t) = f_1(V_1(t), V_2(t), \dot{V}_1(t), \dot{V}_2(t)) \quad (5)$$

$$I_2(t) = f_2(V_1(t), V_2(t), \dot{V}_1(t), \dot{V}_2(t)) \quad (6)$$

The generalized form of this equation for a two-port device is

$$I_1(t) = f_1(V_1(t), V_2(t), \dot{V}_1(t), \dot{V}_2(t), \dot{V}_1(t), \ldots, \dot{I}_1(t), \dot{I}_2(t)) \quad (7)$$

$$I_2(t) = f_2(V_1(t), V_2(t), \dot{V}_1(t), \dot{V}_2(t), \dot{V}_1(t), \ldots, \dot{I}_1(t), \dot{I}_2(t)) \quad (8)$$

The objective of the modeling procedure is to find the functional relationships $f_1(.)$ and $f_2(.)$. Because the black-box modeling approach supposes that no physical background information is available, we first have to determine the independent variables of the functions $f_1(.)$ and $f_2(.)$, which are the state variables. In our method, these state variables are estimated from time domain large-signal measurements. The flowchart of the modeling process is depicted in Figure 2. All steps are described in detail hereafter.

The model is built from time domain data obtained by performing vectorial large-signal measurements using the nonlinear network measurement system (NNMS) [4]. The NNMS works by attempting to accurately reconstruct the large-signal time domain

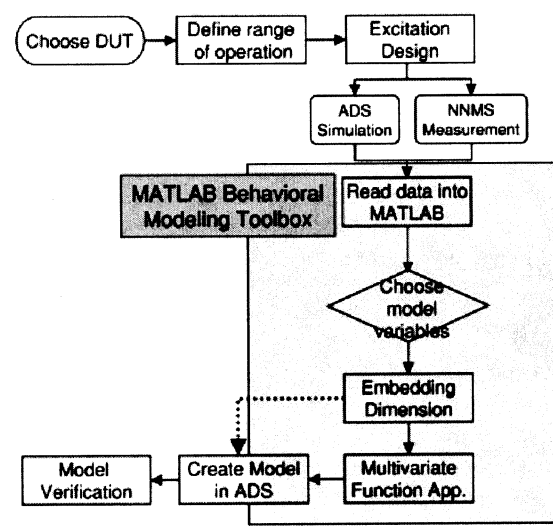

Figure 2. A flowchart of the time domain measurement based behavioral modeling procedure.

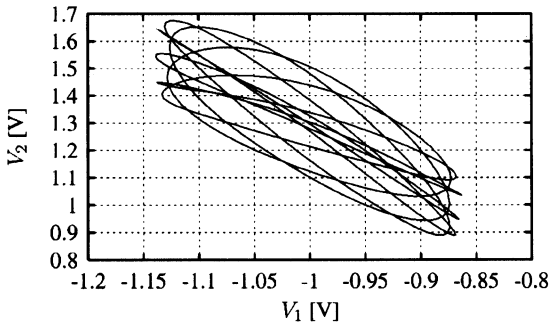

Figure 3. Example coverage of the (V_1, V_2) plane by a *single* vectorial large-signal measurement under two-tone excitation.

voltage waves by measuring the harmonics up to 20 GHz (i.e., the current bandwidth limitation of the system), which are properly amplitude and phased aligned in the frequency domain. The nonlinear time domain signal is then obtained from a Fourier transform to the time domain.

At the start of the modeling process, operating bounds for the model are established by defining the minimum and maximum values of the state variables. These bounds define the operation region within the state space for which the model is to be developed and used. To enable practical identification of the device dynamics, the measured time domain data need to sample this operation region efficiently. However, because the actual state variables are unknown at the start, we begin by defining the minimum and maximum V_1 and V_2 voltages.

The advantage of applying a large-signal excitation to the device instead of the conventional small-signal excitation (bias-dependent *S*-parameters) is that the device is characterized under conditions that are closer to real use. The instantaneous voltage trajectory can sample an extensive region of the device's (V_1, V_2) plane, which is otherwise unreachable by conventional measurements. This is illustrated by Figure 3, in which the time domain waveform of $V_2(t)$ is plotted as a function of the time domain waveform of $V_1(t)$. In this example, the HEMT device was excited by a single tone signal at the gate and by a second periodic signal at a different fundamental frequency at the drain. The (V_1, V_2) area is divided in a grid with 50 mV × 100 mV sections. The purpose of the data gathering process is to have a minimum number of time domain data in each of the sections. For the given example, we notice that one large-signal measurement crosses 28 of these sections. Hence, all the practical (V_1, V_2) area can be sufficiently covered with a minimum number of vectorial large-signal measurements. This can be achieved by suitable variations of the parameters of the measurement system: the DC bias, input powers, input frequencies, and so forth [5]. It is important to point out that the proposed procedure in this work does not require multiple trajectories through exactly the same (V_1, V_2) grid points, which is a requirement for the direct extraction method [5, 7].

We performed similar measurements on an amplifier MMIC. In this case, we measured at the fundamental frequencies covering the amplifier's bandwidth and varied the input powers, because the amplifier's optimal operation fixes the DC bias condition.

The next step is to determine a minimal set of independent variables needed to accurately predict the device dynamics. The initial set of independent variables from which the model is built consists of the measured terminal voltages and currents and their derivatives, as defined in eqs. (7) and (8). We could use all the possible independent variables to an arbitrary fixed order; however, this would result in models that are needlessly complex. A more principled way exists for selecting a subset of independent variables from which to construct a model. This principle, which is from recent developments in NLTSA, generally goes under the rubric of "embeddology" [11]. In practical terms a "good" (although not necessarily unique) subset of independent variables should have the property that a given response current should be a single-valued function of the independent candidate. As described in detail by [14, 15], this is a topological property of the solution sampled by the data and, as such, it should be independent of the model structure. Based on this argument, the authors propose a diagnostic called "false nearest neighbors" to identify a "good" subset of independent variables. In our models we also use the false nearest neighbors test to select the set of independent variables from which to build our models.

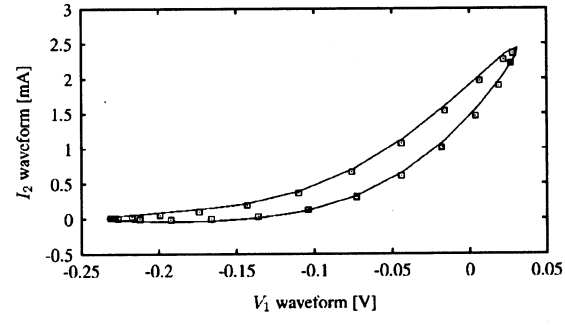

Figure 4. The measured $I_2(t)$ time domain waveform of a HEMT as a function of the corresponding $V_1(t)$ time domain waveform.

TABLE I. Normalized Number of False Nearest Neighbors (FNN) for Currents I_1 and I_2 of the HEMT as Function of the State Variables

Dimension	FNN		State Variables
	I_1	I_2	
3	0.4920	0.4179	$(I_1$ or $I_2) + V_1, V_2$
4	0.2504	0.2494	$(I_1$ or $I_2) + V_1, V_2, \dot{V}_1$
5	0.1202	0.2369	$(I_1$ or $I_2) + V_1, V_2, \dot{V}_1, \dot{V}_2$
6	0.0513	0.1990	$(I_1$ or $I_2) + V_1, V_2, \dot{V}_1, \dot{V}_2, \ddot{V}_1$
7	0.2050	0.3816	$(I_1$ or $I_2) + V_1, V_2, \dot{V}_1, \dot{V}_2, \ddot{V}_1, \ddot{V}_2$

To illustrate the idea, we plotted for a HEMT the time domain waveform of $I_2(t)$ as a function of the time domain waveform of $V_1(t)$ (Fig. 4). We note that $I_2(t)$ is not a single-valued function of $V_1(t)$, which indicates that V_1 is not the only independent variable. In the case of the idealized HEMT [Fig. 1 and eq. (6)], if we would plot this $I_2(t)$ characteristic in a 5-dimensional space, in which the different dimensions are defined by I_2, V_1, V_2, $\dot{V}_1$, and $\dot{V}_2$, we would obtain a single-valued function. Hence, the purpose of embedding the data in a higher dimensional space is to create a space of sufficient dimension so that the dependent variables (I_1, I_2) are single-valued functions of the independent variables $(V_1, V_2, \dot{V}_1, \ldots)$. As the example above illustrates, this is often not the case if we simply use (V_1, V_2) as independent model variables. In order to identify this sufficient set of model variables our method differs slightly from that described in [14, 15], in that we are using derivatives instead of time delay variables. However, our algorithm is the same otherwise. This implies that these embedded models can be faithful to the dynamics of the original system. In particular, deterministic prediction is possible from an embedded model that will mimic the actual dynamics.

The results of applying this technique to actual measured data of the HEMT and amplifier MMIC under study are displayed in Tables I and II. The first column represents the dimensionality of the state space. The numbers in the second and third columns are for I_1 and I_2, respectively, which are the normalized number of data points that have "false" neighbors, which is an indication to check whether a single-valued function can be obtained for that dimensionality of the state space. The last column lists the state variables that have been taken into account for this calculation. When performing measurements at fundamental frequencies up to 5 GHz, we found that it is necessary to include state variables up to $\ddot{V}_1(t)$ for I_1 and I_2 in the case of the HEMT and up to $\dot{V}_1(t)$ for I_1 and $\dot{V}_2(t)$ for I_2 in the case of the amplifier MMIC.

Finally, the functional relationships $f_1(.)$ and $f_2(.)$ of eqs. (7) and (8) are determined by fitting the measured time domain terminal currents, using the independent variables determined in the preceding step. In this work, we use multivariate polynomials to describe $f_1(.)$ and $f_2(.)$, but other types of fitting functions can also be used. A least squares fitting procedure is used to obtain the multivariate polynomial coefficients.

III. RESULTS

We implemented the obtained behavioral models in the Agilent Advanced Design System (ADS) microwave circuit simulator by means of a symbolically defined device (SDD). The SDD can determine the time derivatives of the terminal voltages at each time step in the simulation, hence enabling the functional forms for the currents to be evaluated.

TABLE II. Normalized Number of False Nearest Neighbors (FNN) for Currents I_1 and I_2 of the Amplifier MMIC as Function of the State Variables

Dimension	FNN		State Variables
	I_1	I_2	
3	0.3449	0.3638	$(I_1$ or $I_2) + V_1, V_2$
4	0.0948	0.1444	$(I_1$ or $I_2) + V_1, V_2, \dot{V}_1$
5	0.1534	0.0959	$(I_1$ or $I_2) + V_1, V_2, \dot{V}_1, \dot{V}_2$
6	0.1103	0.1429	$(I_1$ or $I_2) + V_1, V_2, \dot{V}_1, \dot{V}_2, \ddot{V}_1$
7	0.0554	0.0521	$(I_1$ or $I_2) + V_1, V_2, \dot{V}_1, \dot{V}_2, \ddot{V}_1, \ddot{V}_2$

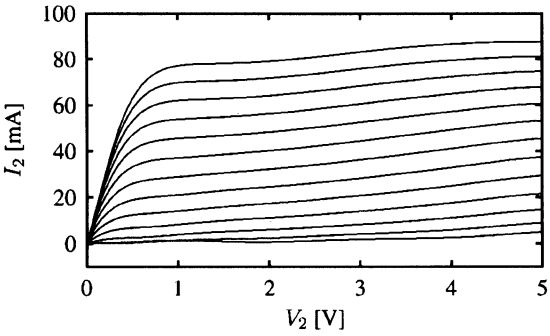

Figure 5. A DC simulation of the dynamically modeled I_2 of a HEMT as a function of V_2 with V_1 ranging between −1.2 and 0 V.

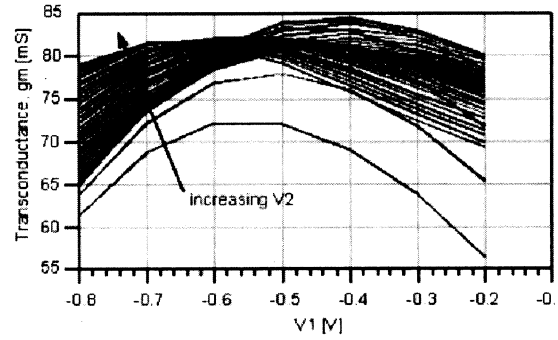

Figure 6. The small-signal g_m value of the HEMT derived from model-generated S-parameters at 20 GHz [V_2 ($=V_{ds}$) = 0.5–4.5 V].

Model validation starts by testing limiting cases, such as a DC or small-signal operation. We note that both DC and small-signal (S-parameters) data were not explicitly used to construct the model. Further validation is achieved by comparing the simulated model performance with measured large-signal data.

The DC I–V characteristics predicted by the HEMT model are shown in Figure 5. The DC behavior of the model arises from effectively setting all the derivative terms to zero in the functional equations for $f_1(.)$ and $f_2(.)$. The resulting I–V curves are then determined by the static nonlinearities in the functions of V_1 and V_2. Figure 5 shows that the dynamical HEMT model provides a good prediction of the static behavior of the HEMT in the region of operation: the results are comparable with our in-house table-based model [16], which is essentially exact at DC, because it is based on measured and interpolated data.

Next, the HEMT behavioral model was used to generate the small-signal S-parameters as a function of the applied DC bias at several frequencies. The HEMT small-signal equivalent-circuit parameters were then extracted using a typical equivalent circuit [17]. In Figures 6 and 7 we show two examples of the small-signal equivalent-circuit parameters: the transconductance (g_m) and the total gate capacitance (C_g). The parameters were extracted at 20 GHz, which is well above the frequencies at which the behavioral model time domain data were measured. The extracted parameters display the general trends of the expected variations with the applied bias as described by the physics of the HEMT. Some capacitive elements, for example, C_{ds}, are less well determined. One of the reasons could be the rather low frequencies that were used in the measurements: the fundamental frequency is less than 5 GHz because of the current bandwidth limitation of the NNMS. This low frequency means that the capacitive component of I_2 is significantly smaller than the in-phase current contributions and that the extraction of this capacitive component is therefore more difficult.

Finally, the model was validated using large-signal measurements. We used the behavioral model to predict the time-dependent output currents $I_1(t)$ and $I_2(t)$ as functions of the drive voltages $V_1(t)$ and $V_2(t)$ and compared the predictions with measured values. The simulations were carried out at the same excitation conditions as the measurements. The input signal was a two-tone excitation with frequencies of 4.0 and 4.5 GHz. Figure 8 presents the excellent agreement between the large-signal simulation and vector-corrected time domain measurements, performed using the NNMS [4], that can be obtained with this new modeling technique.

We conducted similar validations on the behavioral model we obtained for the amplifier MMIC. Figure 9 shows the very good agreement between the large-signal simulation and corresponding measurements under one-tone excitation.

The proposed modeling method is based on large-signal time domain data of the device under test.

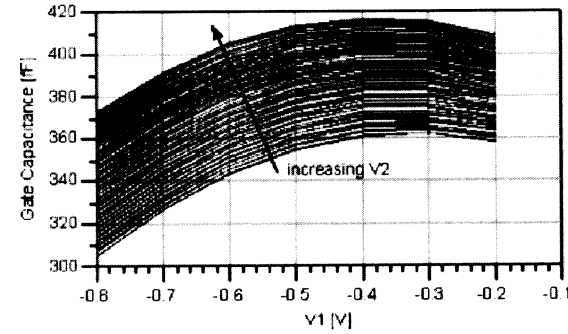

Figure 7. The small-signal C_g value of the HEMT derived from model-generated S-parameters at 20 GHz [V_2 ($=V_{ds}$) = 0.5–4.5 V].

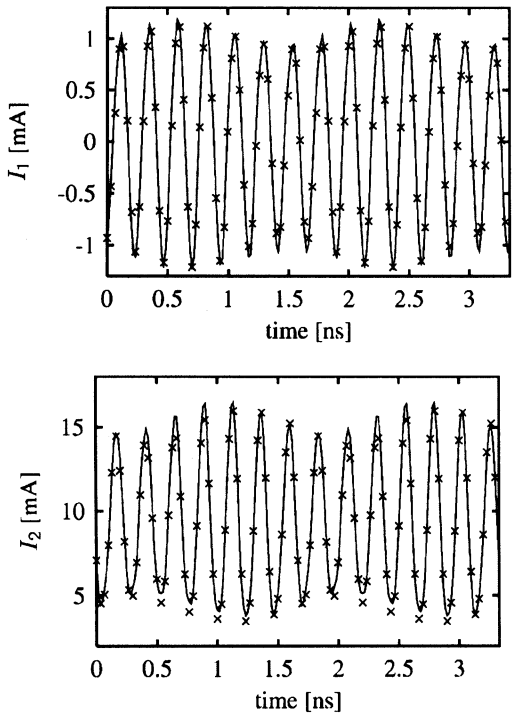

Figure 8. A comparison of the (×) measured and (—) modeled $I_1(t)$ (top) and $I_2(t)$ (bottom) values of a HEMT under two-tone excitation.

These data can be obtained by either performing vectorial large-signal measurements or by simulating a conventional model of the device using harmonic balance or a time domain analysis. Here the terminal voltages and currents and their higher order time derivatives are determined directly in the simulator. The excitation design and model generation process follow the same principles as for the models produced from measured data. In this case the purpose is to also construct a lower dimensional behavioral model of the device for which the validity range is determined by

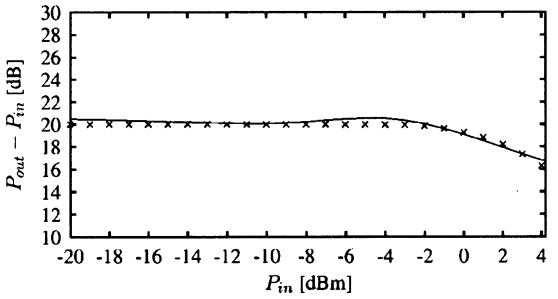

Figure 10. The gain versus the input power of an amplifier MMIC. (×) The simulation results using the transistor-level model for the MMIC; (—) the simulation results of the corresponding behavioral model, obtained without any iteration during the modeling process.

the observable dynamics. The advantage of such lower dimensional behavioral models, especially in the case of circuits, is that the simulation time is significantly reduced compared to the simulation of the full transistor-level representation of the circuit. The gain in simulation speed depends on the circuit's complexity and the type of simulations, but our preliminary results show over a 10-fold reduction in simulation time. This is illustrated by Figure 10, where we compare the simulation results of the behavioral model of an amplifier MMIC with the results of the corresponding full transistor-level model representation. Note that there were no iterations during the process of creating the behavioral model, which implies that there is still room for improvement in the accuracy. This one-cycle model generation took about 2 h, of which the data gathering step, which consisted of simulating the transistor-level model of this MMIC, consumed 75% of the time, the embedding and function fitting took 20%, and the model implementation utilized 5%. The particular power sweep shown in Figure 10 took 140 s in the transistor-level

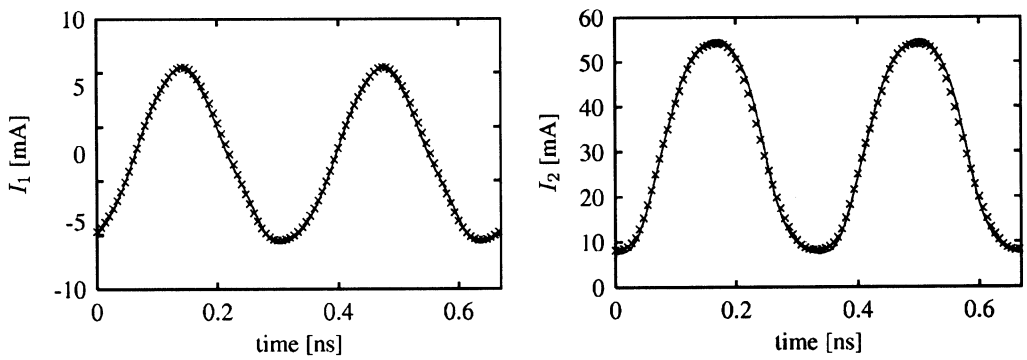

Figure 9. A comparison of the (×) measured and (—) modeled $I_1(t)$ (left) and $I_2(t)$ (right) of an amplifier MMIC at 3 GHz.

model, whereas the behavioral model based simulation only took 14 s. Such an improvement in simulation speed is of great importance when simulating high-level designs, such as (sub)systems, which consist of ICs as building blocks.

IV. CONCLUSIONS

We presented a methodology for developing time domain black-box models for nonlinear microwave devices directly from vectorial large-signal measurements or simulated data. The advantages of this method are that it is not restricted to weakly nonlinear systems and the dynamics of the device are determined directly from the time-series data, resulting in a compact, accurate, and transportable model. The resulting model of the HEMT device shows excellent prediction of large-signal performance and displays physically realistic behavior under the limiting cases of DC and small-signal (linear) conditions. Moreover, we showed that this method is applicable not only to microwave transistors but also to ICs, because no physical preknowledge is required. Because the observable dynamics are determined directly from the large-signal time-series data of the IC, the model does not need to explicitly include the internal, unobservable dynamics of the individual transistors in the IC. This results in a compact model that simulates the IC behavior accurately and quickly.

ACKNOWLEDGMENTS

The first author (D.S.) is supported by the Fund for Scientific Research–Flanders as a Postdoctoral Fellow. This work was performed in the framework of a Visiting Scientist position held by the first author (D.S.) at the Agilent Technologies Microwave Technology Center. We thank the management of Agilent Technologies, Inc. for their support of this work.

REFERENCES

1. F. van Raay and G. Kompa, A new on-wafer large-signal waveform measurement system with 40 GHz harmonic bandwidth, IEEE MTT-S International Microwave Symposium Digest, 1992, pp. 1435–1438.
2. M. Demmler, P. Tasker, and M. Schlechtweg, A vector corrected high power on-wafer measurement system with a frequency range for the higher harmonics up to 40 GHz, Proceedings of the European Microwave Conference, 1994, pp. 1367–1372.
3. C. Wei, Y. Lan, J. Hwang, W. Ho, and J. Higgins, Waveform characterization of microwave power heterojunction bipolar transistors, IEEE MTT-S International Microwave Symposium Digest, 1995, pp. 1239–1242.
4. J. Verspecht, P. Debie, A. Barel, and L. Martens, Accurate on wafer measurement of phase and amplitude of the spectral components of incident and scattered voltage waves at the signal ports of a nonlinear microwave device, IEEE MTT-S International Microwave Symposium Digest, 1995, pp. 1029–1032.
5. D. Schreurs, Overview of non-linear device modeling methods based on vectorial large-signal measurements, Proceeding of the European Gallium Arsenide and Related III–V Compounds Application Symposium, 1999, pp. 381–386.
6. M. Curras-Francos, P. Tasker, M. Fernandez-Barciela, Y. Campos-Roca, and E. Sanchez, Direct extraction of nonlinear FET Q–V functions from time domain large-signal measurements, IEEE Microwave Guided Wave Lett 10 (2000), 531–533.
7. D. Schreurs and J. Verspecht, Large-signal modeling and measuring go hand-in-hand: Accurate alternatives to indirect *S*-parameter methods, Int J RF Microwave Comput Aided Eng 10 (2000), 6–18.
8. J. Verspecht, F. Verbeyst, M. Vanden Bossche, and P. Van Esch, System level simulation benefits from frequency domain behavioral models of mixers and amplifiers, Proceedings of the European Microwave Conference, 1999, pp. 29–32.
9. H. Kantz and T. Schreiber, Nonlinear time series analysis, Cambridge University Press, New York, 1997.
10. J. Hellerstein, "An introduction to modeling dynamic behavior with time series analysis," Performance evaluation of computers and communication systems, Springer–Verlag, New York, 1993, pp. 203–223.
11. M. Casdagli, "A dynamical systems approach to modeling input–output systems," Nonlinear modeling and forecasting, SFI studies in the sciences of complexity, Proceedings, M. Casdagli and S. Eubank (Editors), Addison–Wesley, Reading, MA, 1992, Vol. XII.
12. D. Walker and N. Tufillaro, Phase-space reconstruction using input–output time series data, Phys Rev E 60 (1999), 4008–4013.
13. D. Walker, R. Brown, and N. Tufillaro, Constructing transportable behavioral models for nonlinear electronic devices, Phys Lett A 255 (1999), 236–242.
14. M. Kennel, R. Brown, and H. Abarbanel, Determining embedding dimension for phase-space reconstruction using a geometrical construction, Phys Rev A 45 (1992), 3403–3411.
15. J. Stark, Delay embeddings and forced systems, J Nonlinear Sci 9 (1999), 255–332.
16. D.E. Root, Measurement-based mathematical active device modeling for high frequency circuit simulation, IEICE Trans Electron E82-C (1999), 924–936.
17. G. Dambrine, A. Cappy, F. Heliodore, and E. Playez, A new method for determining the small-signal equivalent circuit, IEEE Trans Microwave Theory Tech 36 (1988), 1151–1159.

BIOGRAPHIES

Dominique M.M.-P. Schreurs received the M.S. degree in electronic engineering and the Ph.D. degree (with honors) from the Katholieke Universiteit (K.U.) Leuven in 1992 and 1997, respectively. She has been a Visiting Scientist at Agilent Technologies (2000), the Swiss Federal Institute of Technology Zurich (2000), and the National Institute of Standards and Technology (2001). She is currently a Postdoctoral Fellow of the Fund for Scientific Research–Flanders and a Visiting Assistant Professor at K.U. Leuven. Dr. Schreurs main research interest is the use of vectorial large-signal measurements for the characterization and modeling of nonlinear microwave devices.

John Wood received the B.S. and Ph.D. degrees in electrical and electronic engineering from the University of Leeds (Leeds, U.K.) in 1976 and 1980, respectively. From 1981 to 1983 he was a Senior Research Engineer with STC Ltd. (U.K.), where he was responsible for GaAs digital IC process development. From 1983 to 1997 he was a member of the academic staff at the University of York (York, U.K.) where he was responsible for teaching and research in solid-state electronics and microwave device and circuit technology. These studies encompassed process development in plasma etching and deposition of metals and silicides, HEMT device modeling, and GaAs field effect transistor (FET) IC design. He is the author or coauthor of over 50 articles. In 1997 he joined the Microwave Technology Center of Agilent Technologies (then Hewlett–Packard) in Santa Rosa, CA. He presently works in the Computer Aided Engineering, Modeling, and Advanced Characterization Group. Dr. Wood's recent research has included the investigation and development of analytical large-signal FET models and bias-dependent linear FET models for millimeter-wave applications, HBT modeling, and behavioral modeling using nonlinear vector network analyzer measurements and nonlinear system identification techniques.

Nick Tufillaro has worked as a Research and Development Scientist and Engineer at Agilent Technologies (formerly Hewlett–Packard) for the last 5 years doing advanced modeling of new RF, microwave, and optical devices, as well as laying the foundations for a general test and measurement methodology for the characterization and design of systems exhibiting nonlinear behavior. Prior to his work at Agilent he performed experimental work on spatial temporal chaos in surface waves, theoretical work in the topological characterization of low dimensional chaos, and developed the first industrial photoluminescence system used in the large-scale production of semiconductor lasers. This work, which was done early in his career while working at Bell Labs, helped to enable TAT-8, the first transatlantic fiber optic cable. He has also worked as a consultant for DOW Chemical, Ford Motor Company, and Hewlett–Packard Company on issues of nonlinear system identification, modeling, and analysis. His research covers a broad area of industrial, applied, experimental, and theoretical physics. A main theme in his work is the analysis and modeling of nonlinear behavior with a strong inclination toward the methods of computational science. Most of the engineering applications of his work are geared toward the high-speed wireless and optical communications industries. Lastly, Mr. Tufillaro is an advocate of free software, to which he has contributed. He is one of the two principal developers of the GNU plotutils package.

Lee Barford. Photo and biography not available.

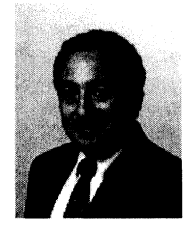

David E. Root is presently Research and Development Project Manager at the Agilent Microwave Technology Center and Lead Modeling Scientist at the Nonlinear Foundations Program at Agilent Technologies (formerly Hewlett–Packard) in Santa Rosa, CA. Since joining Hewlett–Packard in 1985, he has held a number of scientific and management positions. He received B.S. degrees in physics and mathematics and the Ph.D. degree in (theoretical) physics, all from MIT. Dr. Root has authored or coauthored more than 60 technical publications. He presented the first charge-based active-capacitance large-signal GaAs MESFET model for SPICE. He originated and codeveloped the commercial HP measurement-based large-signal "Root" MESFET/HEMT, metal oxide FET, and diode models, model generators, and associated automated data acquisition systems, for which he received a U.S. patent. He originated and codeveloped DMYSTFY, a nonparametric statistical simulation and design methodology, and applied it to IC manufacturability. From 1997 to 2001 Dr. Root managed the Agilent Microwave Technology Center computer-aided engineering, modeling, and advanced characterization group. He managed the establishment of state of the art nonlinear measurement capability in the advanced characterization lab. This included novel systems for fast, pulsed bias and pulsed *S*-parameter characterization, automated high dynamic range distortion measurements, a prototype vectorial nonlinear network analysis system, and a system for high-speed time domain characterization. Simultaneously, he managed device modeling for several Agilent FET, diode, and heterojunction bipolar semiconductor processes, and the development, customization, and support of microwave design tools. Recent work with his team, including visiting researchers, has involved nonlinear behavioral modeling using waveform data and mathematical techniques of nonlinear dynamics. Dr. Root serves on the editorial board of the IEEE Transactions on Microwave Theory and Techniques and the technical program committee of the IEEE International Microwave Symposium. He is a Fellow of the IEEE.